Liner Plate Design Considerations for the Tsuruga Unit No. 2 Power Station

M. Uchiyama, H. Yamaguchi
The Japan Atomic Power Company, Tokyo 100, Japan
T. Suzuki
Mitsubishi Heavy Industries, Ltd., Takasago Technical Institute, Takasago 676, Japan
K. Nagata
Mitsubishi Heavy Industries, Ltd., Kobe Shipyard and Engine Works, Kobe 652, Japan
D.Z.F. Deng, B.W. Wedellsborg
Bechtel Power Corporation, P.O. Box 3965, San Francisco, California 94119, U.S.A.

ABSTRACT

The paper summarizes the joint activities of Bechtel, JAPC and MHI on the design, test, and research on the liner-anchor system for JAPC's Tsuruga Unit No. 2 Power Station (PWR). The containment structure is a prestressed concrete cylinder shell with hemispherical dome. The entire liner-anchor system was designed to maintain the leak-tight integrity of the containment.

The anchoring system is a continuous orthogonal gridwork of rolled structural shapes including flat bars, tees and angles. The liner anchor system is designed to resist severe design wind load condition during liner erection and is used as construction form during concrete placement. The strain is imposed on the liner-anchor system by deformation of concrete containment. This deformation is caused by all potential normal operating conditons and severe accidental condition, e.g. temperature and pressure rises caused by LOCA incident, and seismic load. Sustaining loading conditions such as concrete creep and shrinkage, in addition to locked-in stress due to concrete placement are also considered. The strain distributions in the liner plate for the imposed loading conditions are presented.

A series of tests were conducted to determine the load-deflection relationship of the embedded liner anchors. The test results provide information for the response analysis of the liner-anchor system cuased by an unbalanced force acting on the anchor. The test setup of the liner anchor specimen and sets of representative test results are presented for different types of anchors. Bilinear relationship between force and anchor displacement are derived by simplified analytical models and compared with the test results.

The analytical model assumes that a row of panels are initially bent inward and the rest of the panels are assumed to remain flat and not deflect laterally so that a maximum in-plane force could be exerted on the anchor. A simple multiple-spring mathematical model is developed to analyze the liner anchor response due to the unbalanced shear force. The stiffness of the anchor, bent panel and the flat panels are simulated by a set of bilinear spring coefficients in the mathematical model. The final stable configuration of the liner-anchor system is obtained by a few cycles of iteration on the governing equilibrium equations. Examples of computed results are discussed.

1.0 INTRODUCTION

The containment structure for the Japan Atomic Power Company's Tsuruga Unit No. 2 Power Station (PWR, 1100 MW) is a prestressed concrete cylinder shell with a hemispherical dome. The liner plate, attached to the inside face of the concrete containment, is anchored to the concrete by the continuous orthogonal gridwork of rolled structural shapes including flat bars, tees, and angles.

The liner plate system was designed with different layouts for floor, cylinder, and dome portions, Figure 1. The floor is composed of 6.4 mm SGV 42 plate, a mild carbon steel, welded to embedded beams. The floor is covered with a concrete slab of minimum 500 mm thickness. A leak-chase system is located over all liner plate seams which are encased in the concrete floor slab. The cylinder is fabricated from 6.4-mm SGV 42 plate together with SM 41 B meridional stiffening tee sections welded to the liner, and SM 41 B flat plates in the hoop direction welded to the liner plate and tee shapes. The rolled structural shapes and flat bars stiffen the liner plate during erection and concrete placement, and anchor the liner plate to the hardened concrete. The dome is similar to the cylinder except that the stiffening system is composed of bars, tee, and angle stiffeners which also act as anchors. The angles are oriented in the hoop direction.

2.0 DESIGN CONDITIONS

The loads considered in the liner plate design cover construction, normal operation, and accident conditions. The construction schedule required that the liner-anchor system be installed with panels of larger than conventional size, and be erected to the spring-line level before concrete placement with minimum construction bracing of the liner-anchor system. The embedded anchors have to conform with the concrete media because their stiffness is relatively less compared with that of the concrete vessel. Hence, the deformation induced in the concrete vessel for the design loads is imparted to the liner-anchor system.

2.1 Loads During Construction Stage

The liner plate is designed to resist all applicable loads and load combinations during erection including dead load, live load, and concrete placement pressure. The concrete placement pressure is derived from semi-hydrostatic type pressure due to wet concrete. The construction loading conditions result in strains remaining locked into the liner plate system for the life of the plant. The construction locked-in strain (ε_c) imposes a negligible unbalanced force on a liner anchor. It is combined with other design loads for the consideration of code-allowed maximum strain of the liner plate.

The liner-anchor system was also designed to resist a strong wind load for two stages of erection: (1) before each tier forms a complete ring structure, and (2) after the cylinder liner is erected to spring line level without concrete placement in the cylinder wall. Current designed layout showed that a maximum lift of 9-m per tier of the liner installatior is possible, and no additional wind bracing is needed if the cylinder liner is erected to spring line level prior to concrete placement.

2.2 Loads During Normal Operation

The significant loadings imposed on the liner-anchor system during normal plant operation and shutdown include dead load, prestress loads, concrete creep and shrinkage strains, normal operating thermal loads, structural integrity testing (SIT) pressure, and construction locked-in strains.

a. Prestress Load (F)

The liner plate is subjected to the induced strain due to the prestress load applied to the PCCV concrete. Long-term stresses due to prestress loads diminish slightly due to creep and shrinkage.

b. Concrete Creep and Shrinkage Strains (ε_{cs})

The combined effects of concrete creep and shrinkage of the PCCV concrete increase the liner plate compressive strains. Creep and shrinkage loads are considered together as a single imposed load on the liner, and are calculated as a function of concrete compressive stress and prestress tendon tensile stress. The most critical condition is near the end of the design life of the structure when the maximum values of creep and shrinkage have been reached.

c. Normal Operating Thermal Load (T_1)

The normal operating temperature inside the containment is about 40°C, and 0°C outside during the winter. This temperature differential induces strains within the concrete and the liner plate.

d. SIT Pressure (P_o)

Before the plant is started for commercial operation, the PCCV is tested for structural integrity by pressurizing the containment to 1.15 times the design accident pressure (P_2).

2.3 Loads for Accident Conditions

The significant loads imposed on the liner-anchor system in the postulated accidental environment include LOCA thermal load, LOCA pressure, and seismic loads for both normal operating basis earthquake (S1) and safe shutdown earthquake (S2).

a. LOCA Thermal Load (T_2)

Under the postulated LOCA condition, the temperature inside the PCCV is calculated to rise to 144°C, which causes a thermal gradient across the concrete wall. Therefore, a thermal strain is induced in the concrete, which is also imparted to the liner plate. Additional thermal strain is produced in the liner plate due to the temperature difference between the inner face of the concrete wall and the liner plate. The temperature in the liner plate is assumed to be equal to the postulated accident temperature of 144°C.

b. LOCA Pressure (P_2)

During the LOCA accident, the internal pressure in the PCCV is calculated to rise to 39.2 N/cm^2, imposing tensile stresses and strains on the liner plate.

c. Seismic Loads (S1, S2)

The design value of the horizontal ground acceleration is 300 gals and 500 gals for S1 and S2 conditions, respectively. The corresponding design value for the vertical ground acceleration is 150 gals and 250 gals.

2.4 Design Load Combination

The load combinations for the design of liner plate system are shown in Table 1. They are classified into four load categories based on the probability of occurrence of the specific events. Load Category I specifies the event during normal operation of the plant. Load Category II includes test load in addition to the normal operating condition. Load Category III specifies loads in S1 earthquake or LOCA conditions. Load Category IV specifies loads in S2 earthquake or S1 earthquake plus LOCA conditions.

The strains of the combined loads were calculated by a non-linear computer program for concrete design, encountering concrete yielding and cracking, and reinforcement yielding. Table 2 presents the calculated distribution of longitudinal membrane strain (ε_x) and circumferential membrane strain (ε_ϕ) induced in the liner plate for each combined loading case, excluding the construction locked-in strains. The corresponding locations are shown in Figure 2. The strains shown in Table 2 show a slightly irregular distribution at some locations which could be attributed to the structural layout, e.g. arrangement of tendon buttresses of the PCCV, location of PCCV penetrations, and distribution of concrete wall reinforcing.

3.0 LINER ANCHORAGE CAPACITY

A series of tests were conducted to determine the load-deflection relationship of liner anchor embedded in the concrete media.

3.1 Test Specimen and Test Setup

The test setup of the liner-anchor specimens is shown in Figure 3. The concrete blocks are 30 cm wide, 150 cm long, and 60 cm high. The dimension of the plate are 30 cm wide, 200 cm long, and 0.64 cm thick. The anchor shapes include CT 129 x 146 x 6 x 9, L 125 x 75 x 7 (both leg-up and leg-down of applied load direction), and PL 12 x 150. Two tie bars were provided to simulate the two-way behavior of the liner-anchor system provided by the end support conditions of the anchor and the embedding concrete media. This arrangement prevents an excessive rotation of the anchor which caused an unreasonable premature failure of the specimen without tie bars.

The concrete strength of the test specimen is about 4300 N/cm^2, and the yield strengths of the liner plate and the anchors are 310 N/mm^2 and 320 N/mm^2, respectively. The load applied to the test specimen was a tensile force through hydraulic rams mounted in a horizontal position. Some specimens were applied with nominal prestress forces of 818 N/cm^2 for Tee, 532 N/cm^2 for Angle and 483 N/cm^2 for plate anchors to simulate the prestressing forces applied to the containment structure.

3.2 Test Results and Design Curves

Sets of representative test results are presented in Figure 4 for four different types of anchors. All tests showed that the liner anchor reaches the maximum shear load capacity prior to the maximum displacement. The tests also showed that there is no significant difference in the load-displacement relationships between prestressed and non-prestressed specimens. However, the final concrete cracking patterns between these two specimens are quite different, Figure 5.

A design curve for each type of anchor was derived theoretically for use of liner-anchor design and analysis prior to performance of testing. For simplicity of analysis, a bilinear relationship between force and anchor displacement was assumed, as shown in Figure 4. Within the initial stage of the design curve, the whole liner-anchor system (including concrete media) is within the elastic range of the system. In the second stage, the liner-anchor system is assumed to deform plastically. The cut-off point was set by assuming that the maximum angle of rotation in the anchor web equal to 16° at the vicinity of welding connection with the liner plate. The anchor displacements at yield and ultimate, and their corresponding shear strengths, are indicated in Figure 4.

The later test results showed that the test curves well envelop the theoretical design curves. Therefore, the anchorage system design based on the theoretical design curves provides a substantial safety margin in regard to the structural integrity of the liner-anchor system.

4.0 ANALYTICAL MODEL FOR EVALUATION OF LINER ANCHORAGE

Some liner panels may be initially bent inward and pose a weaker stiffness than that of the adjacent panels in resisting the in-plane force. In this case, an unbalanced force would be exerted on the anchor at the juncture of these two panels. The bent panel would then bend further inward and the adjacent panel would be able to release some of the strain imposed by the loadings.

4.1 Mathematical Model for Liner-Anchor Response

A finite element mathematical model was developed to analyze the liner-anchor response due to the unbalanced force as shown in Figure 6. The analytical model assumes that a row of panels are initially bent inward and the rest of the panels are assumed to remain flat which would not deflect laterally so that a maximum in-plane force could be exerted on the anchor. The postulated model simulates a strip of unit width cut at the mid-panel line from pertinent numbers of panels. The components and their respective stiffnesses are presented as follows:

a. Anchors

The i^{th} anchor away from the bent panel is depicted by a spring represented by a pair of spring coefficients C_i and C_{ip} representing elastic and plastic deformations, respectively, of the anchor. The idealized bilinear curves based on analytical results, shown in Figure 4, are used for the computation of C_i and C_{ip}.

b. Bent Panels

The bent panel is represented by a spring with spring coefficients of B and B_p for elastic and plastic deformation, respectively. The force-displacement relationship of the bent panel is also depicted as a bilinear curve based on test data. The test specimen was a steel plate 15.2 (wide) x 61 (long) x 0.64 cm (thick) fixed at both ends. The plate was pre-bent to a 1.3 cm deflection at the center and then an axial load was applied to the ends. The test results and the corresponding simplified bilinear design curve is shown on Figure 7.

c. Flat Panels

The flat panels are represented by a pair of springs with spring coefficients of βR_1 and $(1-\beta)R_1$. The former represents the stiffness due to axial deformation (in-plane) of the panel and the latter represents the shear stiffness of the panel. The panel stiffnesses were derived based on two-dimensional behavior of the panel as depicted in Figure 8, where β is the carry-over factor representing the ratio of force in the rear edge (F_r) to that of the front edge (F_f) where the force is applied, and R_1 is the ratio of the applied force to the corresponding displacement at the front edge. The values of β and R_1 as functions of the rectangular panel aspect ratio were computed based on the simplified analytical model developed by Wedellsborg, [1].

A bilinear force-displacement relationship was utilized for the liner panel. After the liner panel reached the yield limit, which was determined by Mises' yield criterion, an ideal rigid plastic stress-strain relationship was assumed.

4.2 Equilibrium Conditions

The final stable configuration for the liner-anchor system subject to the unbalanced force at one anchor can be obtained by solving the following governing equilibrium equations:

$$F_o + A_1 + S_1 = F_1 \qquad \text{at Node No. 1} \qquad (1)$$

$$F_{i-1} + A_i + S_i = F_i \qquad \text{at Node No. i}$$

where F_o = axial force in bent panel, A_1 = force at 1st anchor, S_1 = shear force in 1st panel, F_1 = axial force in 1st panel, F_{i-1} = axial force in $(i-1)^{th}$ panel, A_i = force at i^{th} anchor, S_i = shear force in i^{th} panel and F_i = axial force in the i^{th} panel.

The force in each element of Equation (1) is expressed in detail in the Appendix. After a few cycles of iteration on the equation, with sufficient numbers of anchors and liner panels used in the model, the final stable configuration of the liner-anchor system could be obtained simply by manual computation.

4.3 Examples

By applying the analytical model described previously, the response of the liner-anchor system is examined for the most critical loading case extracted from Table 2. Analytical results of two examples on the cylinder liner will be presented briefly herein. The basic geometrical and mechanical characteristics of the liner panel and anchor are presented as follows:

Anchor type:	CT 129 x 146 x 6 x 9 mm
Anchor Spacing:	Meridional anchor = 60 cm
	Hoop anchor = 260 cm
Bent panel elastic spring constant:	$B = 12700$ N/cm^2
Bent panel plastic spring constant:	$B_p = 1270$ N/cm^2
Bent panel displacement at yield :	$U_B = 0.125$ cm
Anchor elastic spring constant :	$C_1 = C_i = 235000$ N/cm^2
Anchor plastic spring constant :	$C_{1p} = C_{ip} = 15700$ N/cm^2
Anchor displacement at yield :	$U_{1d} = U_{id} = 0.032$ cm
Anchor Ultimate Displacement :	$U_{ult} = 0.85$ cm

Case 1 Normal Operating Condition

The most critical strains imposed in the liner panel for normal operating condition are:

$$\varepsilon_x = -982 \times 10^{-6}$$

$$\varepsilon_\phi = -1270 \times 10^{-6}$$

for axial and circumferential directions, respectively. After 2 cycles of iteration, the final stable anchor displacement is obtained as 0.093 cm at the first anchor, which is about 0.11 times of the design maximum anchor displacement. The stress in the first panel, after relaxation, is reduced to -13300 N/cm^2, compared with the maximum of -35700 N/cm^2 for panels subjected to the same biaxial strain input without relaxation.

Example 2 Accident Condition

Loading case No. 8 with LOCA plus S_1 earthquake conditions results in the most cricitical strains in the liner panel which are

$$\varepsilon_x = -1979 \times 10^{-6}$$

$$\varepsilon_\phi = -2097 \times 10^{-6}$$

at location No. 5. After 6 cycles of iteration, the final stable anchor displacement was obtained as 0.154 cm at the first anchor, which is about 0.18 times the design maximum

anchor displacement. The stress in the first panel, after relaxation, is reduced to -23700 N/cm^2, compared with the maximum of -34700 N/cm^2, for panels subjected to the same biaxial strain input without relaxation.

Reference

[1] Wedellsborg, B.W., "Two-Dimensional Nonlinear Analysis of Steel Liner and Anchorage Systems for Post-Tensioned Concrete Containment Buildings," Sixth International Conference on Structural Mechanics in Reactor Technology, Paris, France; Paper J 3/4, August 1981.

APPENDIX

The functions shown in Equation (1) can be expressed in terms of singularity functions as:

$$F_o = BU_1 \langle U_B - U_1 \rangle^0 + BU_B \langle U_1 - U_B \rangle^0 + B_p \langle U_1 - U_B \rangle^1$$

$$A_1 = C_1 U_1 \langle U_{1d} - U_1 \rangle^0 + C_1 U_{1d} \langle U_1 - U_{1d} \rangle^0 + C_{1p} \langle U_1 - U_{1d} \rangle^1$$

$$S_1 = (1-\beta) R_1 U_1$$

$$F_1 = [N_1 - \beta R_1 (U_1 - U_2)] \langle N_p - N_1 + \beta R(U_1 - U_2) \rangle^0 + N_p \langle N_1 - N_p - \beta R(U_1 - U_2) \rangle^0$$

$$F_{i-1} = [N_{i-1} - \beta R_1 (U_{i-1} - U_i)] \langle N_p - N_{i-1} + \beta R(U_{i-1} - U_i) \rangle^0 + N_p \langle N_{i-1} - N_p - \beta R(U_{i-1} - U_i) \rangle^0$$

$$A_i = C_i U_i \langle U_{id} - U_i \rangle^0 + C_i U_{id} \langle U_i - U_{id} \rangle^0 + C_{ip} \langle U_i - U_{id} \rangle^1$$

$$S_i = 2(1-\beta) R_1 U_i$$

$$F_i = [N_i - \beta R_1 (U_i - U_{i+1})] \langle N_p - N_i + \beta R(U_i - U_{i+1}) \rangle^0 + N_p \langle N_i - N_p - \beta R(U_i - U_{i+1}) \rangle^0$$

where

U_i = Final displacement at i^{th} anchor

U_{id} = Anchor displacement at yield for i^{th} anchor

N_i = Imposed initial unrelaxed hoop force in i^{th} panel

N_p = Force in panel at yielding limit.

The function $\langle x-a \rangle^0$ is defined as unit step starting at x = a and the function $\langle x-a \rangle^1$ is defined as unit ramp starting at x = a which can be depicted as the following figures:

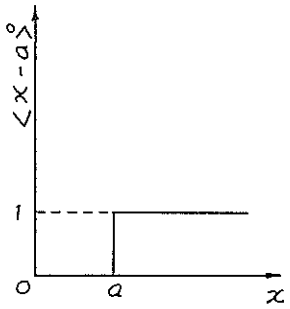

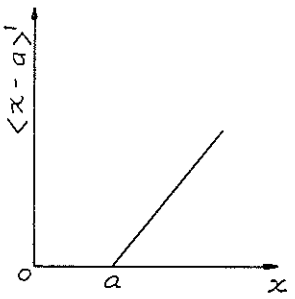

TABLE I

LOAD COMBINATION FOR LINER PLATE SYSTEM

LOAD CATEGORY	NO.	LOAD COMBINATION	LOAD FACTORS D DEAD LOADS	F PRESTRESS LOAD	T_1 NORMAL OPERATING THERMAL LOADS	P_0 TEST PRESSURE	P_2 ACCIDENT PRESSURE	T_2 ACCIDENT THERMAL LOADS	K_1 S_1 EARTHQUAKE	K_2 S_2 EARTHQUAKE	ϵ_{cs} CREEP AND SHRINKAGE	ϵ_c** CONSTRUCTION
I	1	NORMAL OPERATING CONDITION	1.0	1.0	1.0						1.0	1.0
II	2	TESTING CONDITION	1.0	1.0		1.0						1.0
III	3*	S_1 EARTHQUAKE CONDITION	1.0	1.0	1.0				1.0		1.0	1.0
	4**	S_1 EARTHQUAKE CONDITION	1.0	1.0	1.0				1.0			1.0
	5	L ACCIDENT CONDITION	1.0	1.0			1.0	1.0			1.0	1.0
IV	6*	S_2 EARTHQUAKE CONDITION	1.0	1.0	1.0					1.0	1.0	1.0
	7**	S_2 EARTHQUAKE CONDITION	1.0	1.0	1.0					1.0		1.0
	8*	L ACCIDENT PLUS S_1 EARTHQUAKE CONDITION	1.0	1.0			1.0	1.0	1.0		1.0	1.0
	9**	L ACCIDENT PLUS S_1 EARTHQUAKE CONDITION	1.0	1.0			1.0	1.0	1.0			1.0

* The combination case is for compressive strain due to seimic loading.

** The combination case is for tensile strain due to seismic loading.

*** The construction strain is used in checking against the code allowable maximum strain in the liner panel but is not used in anchor displacement computation.

TABLE II

COMBINED MEMBRANE STRAIN DISTRIBUTION (x 10^{-6})

Load No.	Axis of Strain	Location No. (See Figure 2) 1	2	3	4	5	6	7	8	9	10	11	12
1	ϵ_x	-1174	-1171	-1174	- 982	- 982	- 990	- 935	- 949	- 965	-1052	-1049	-1049
	ϵ_ϕ	- 895	- 899	- 897	-1158	-1270	-1106	-1251	-1227	-1214	-1181	-1148	-1157
2	ϵ_x	- 109	- 113	- 110	- 82	- 82	- 91	- 85	- 95	- 98	- 142	- 131	- 133
	ϵ_ϕ	- 4	- 7	- 6	- 52	- 52	- 51	- 41	- 51	- 49	- 78	- 91	- 89
3	ϵ_x	-1202	-1214	-1407	-1097	-1048	- 802	-1021	-1007	- 851	-1070	-1014	- 945
	ϵ_ϕ	-1018	-1027	- 851	-1086	-1308	-1183	-1135	-1272	-1227	-1062	-1136	-1180
4	ϵ_x	- 574	- 574	- 788	- 460	- 156	- 136	- 390	- 177	- 220	- 464	- 375	- 347
	ϵ_ϕ	- 254	666	431	- 322	- 363	- 432	- 363	- 335	- 472	- 308	- 350	- 435
5	ϵ_x	-1797	-1760	-1775	-1820	-1823	-1783	-1786	-1764	-1780	-1766	-1759	-1761
	ϵ_ϕ	-1761	-1764	-1761	-1821	-1866	-1815	-1808	-1820	-1806	-1828	-1829	-1832
6	ϵ_x	-1219	-1333	-1300	-1104	-1053	- 815	-1032	-1018	- 869	-1064	-1012	- 950
	ϵ_ϕ	-1034	-1043	- 878	-1117	-1330	-1216	-1138	-1265	-1226	-1068	-1138	-1176
7	ϵ_x	- 585	- 619	- 765	- 465	- 143	- 133	- 399	- 181	- 231	- 458	- 378	- 353
	ϵ_ϕ	- 271	848	527	- 352	- 388	- 469	- 368	- 342	- 474	- 313	- 356	- 431
8	ϵ_x	-1863	-1867	-1964	-2043	-1979	-1426	-1964	-1920	-1668	-1851	-1797	-1721
	ϵ_ϕ	-1962	-1932	-1496	-1799	-2097	-1905	-1661	-2045	-1974	-1664	-1886	-1956
9	ϵ_x	-1250	-1126	-1334	-1411	- 326	- 78	-1311	- 677	- 973	-1224	-1103	-1102
	ϵ_ϕ	-1184	420	202	- 964	- 698	-1283	-868	887	-1214	- 887	-1057	-1214

Note: The combined strains include the strains induced by all loads except the construction loads for the corresponding loading case.

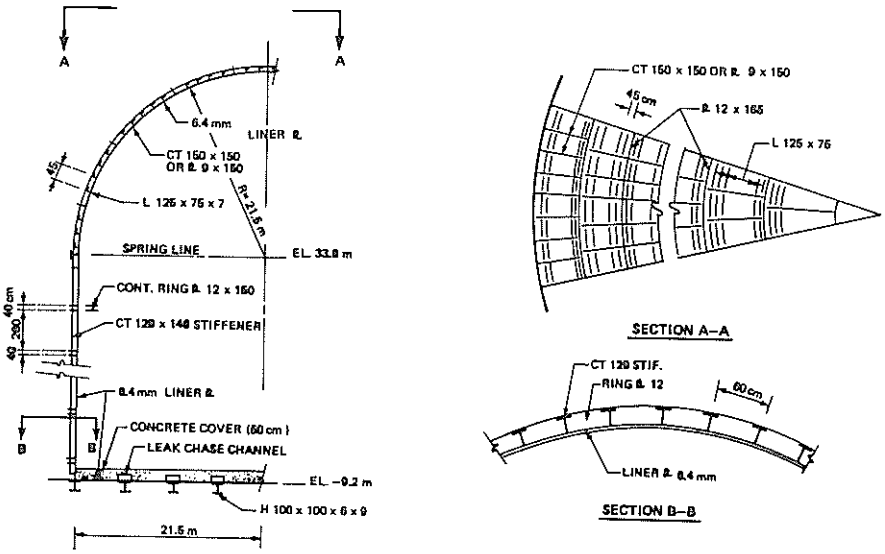

FIGURE 1 LINER–ANCHOR SYSTEM

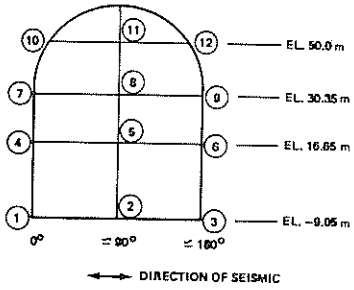

FIGURE 2 LOCATIONS WITH LINER STRAINS SHOWN IN TABLE 3

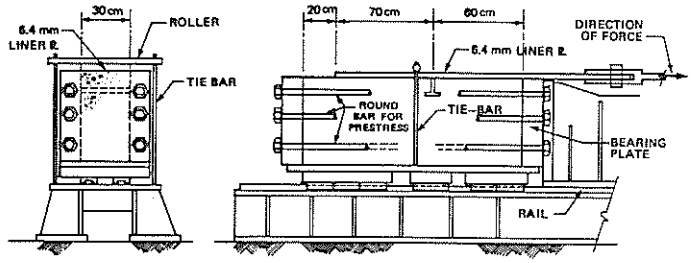

FIGURE 3 SHEAR TEST SPECIMEN AND TEST SET–UP

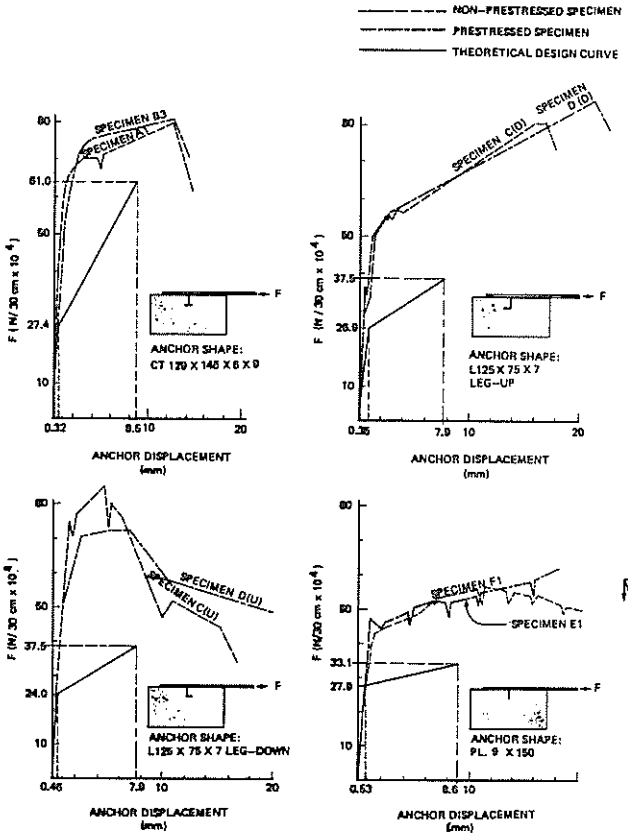

FIGURE 4 FORCE–DISPLACEMENT CURVES

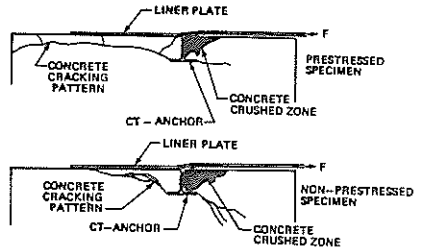

FIGURE 5 COMPARISON OF FAILURE MODES OF PRESTRESSED & NON-PRESTRESSED SPECIMENS

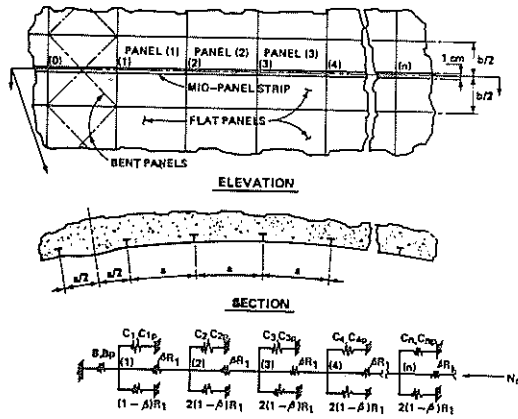

FIGURE 6 TWO–WAY LINER MATHEMATICAL MODEL

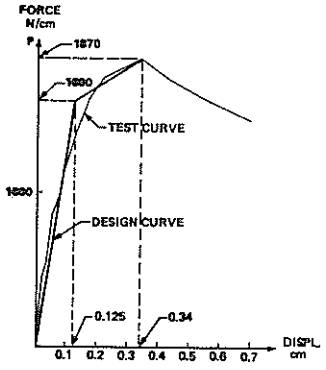

FIGURE 7 DESIGN CURVE FOR BENT PANEL

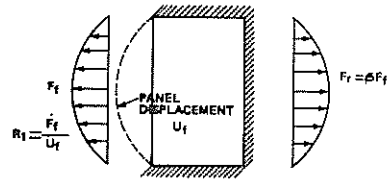

FIGURE 8 FLAT PANEL SUBJECT TO IN–PLANE LOADING